

Photon echoes and free-polarization decay in GaAs/AlAs multiple quantum wells: Polarization and time dependence

Harald Schneider

Fraunhofer-Institut für Angewandte Festkörperphysik, Tullastrasse 72, D-79108 Freiburg, Germany

Klaus Ploog*

Max-Planck-Institut für Festkörperforschung, Heisenbergstrasse 1, D-70506 Stuttgart 80, Germany

(Received 27 January 1994)

We have studied picosecond two-pulse degenerate four-wave mixing in GaAs/AlAs quantum wells under different polarization configurations of the two pump beams and the analyzed optical polarization. We observe two components, a prompt free polarization decay (FPD) and a delayed photon echo (PE), which show different polarization rules and dephasing times. The observed polarization rules are consistently explained in a theoretical model. Within this model, the two-component behavior is a direct consequence of short-range disorder. The PE dephasing rate is associated with the homogeneous broadening of the excitons while the FPD corresponds to the total dephasing rate, consisting of the homogeneous and inhomogeneous (short-range and long-range) broadenings.

I. INTRODUCTION

Degenerate four-wave mixing (DFWM) has proven to be a powerful method to analyze the coherent properties of excitons in bulk semiconductors and quantum wells (QW's).¹⁻²⁰ In particular, DFWM provides an experimental approach to the investigation of scattering processes of excitons with excitons,² acoustic phonons,^{3,4} and free carriers,^{5,6} limiting the excitonic coherence. The observation of quantum-beat phenomena in QW's (Refs. 7 and 8) has again proven the significance of the method, e.g., in providing new information on the physics of resonant tunneling.⁹ Application of DFWM to doped systems⁶ allows us to study the coherence of free electrons or holes. These studies have been performed in a two-pulse¹⁻¹⁷ or three-pulse¹⁶⁻²⁰ DFWM configuration. In two-pulse DFWM, copolarized^{1,5,6} or cross-polarized^{6-10,16,17} light pulses of wave vectors $\mathbf{k}_1, \mathbf{k}_2$ are incident on the sample, giving rise to a signal detected in the diffracted direction $2\mathbf{k}_2 - \mathbf{k}_1$.

Only very recently has the influence of the particular polarization configuration on the DFWM signal been studied in more detail. Schmitt-Rink *et al.*¹² and Eccleston *et al.*¹³ have reported a phase reversal of DFWM quantum beats between heavy- and light-hole excitons of 17- and 27-nm-wide GaAs multiple QW's, respectively, on changing from copolarized to cross-polarized excitation. Simultaneously, a polarization dependence of the measured dephasing times has been found¹² at exciton densities below a certain crossover density ($< 10^9 \text{ cm}^{-3}$), in conjunction with an intensity-dependent variation of the apparent DFWM polarization rules.¹³ Only the high-intensity DFWM signal was observed to satisfy the polarization rules expected theoretically^{12,14} for free-exciton dephasing.¹³ The influence of disorder on the polarization rules has been described by Bennhardt *et al.*¹⁴ in a phenomenological model, which correctly explains

the dependence of the apparent dephasing times on the exciting field polarizations.

Strongly polarization-dependent excitonic nonlinearities have been observed by Cundiff, Wang, and Steel¹⁹ in 10-nm GaAs multiple QW's, with a factor of typically 10 between the dephasing rates under copolarized and cross-polarized excitation. It was also shown that low-intensity copolarized and cross-polarized excitations give rise to a delayed signal [or photon echo (PE)] and to a prompt signal [or free-polarization decay (FPD)], respectively. Since the delayed signal saturates at a smaller intensity than the prompt one,¹⁹ a two-component behavior of the DFWM signal has been observed under appropriate conditions.²⁰ These results have been attributed to a homogeneously broadened population of delocalized excitons and an inhomogeneously broadened population of excitons localized by interface roughness, giving rise to the FPD and PE signals, respectively.²⁰ This interpretation is consistent with the observed saturation behavior. It also explains the observation that the delayed signal is associated with a smaller excitonic mobility than the prompt one.¹⁹

In this work, we report on the systematic investigation of the polarization rules of different components of the DFWM signal caused by heavy-hole excitons in GaAs QW's. For copolarized excitation, the signal of the two-pulse DFWM experiment consists of two components, namely, a PE which is time delayed with respect to the second pump pulse, and a prompt FPD. We have time separated the PE component with a streak camera and analyzed its polarization rules. The PE polarization is found to coincide essentially with the polarization of the *second* excitation pulse. The polarization rules of the FPD signal have been determined under 45° polarization angle between the excitation pulses. Our results are correctly explained within the model of Bennhardt *et al.*,¹⁴ and a generalization of this model is proposed.

II. EXPERIMENT

The samples used in our experiments are undoped multiple QW structures consisting of 50 periods of 12.3-nm GaAs/2.1-nm AlAs (sample *A*) and 11.8-nm GaAs/1.6-nm AlAs (sample *B*), respectively, forming the intrinsic layer of a *p-i-n* diode.²² The samples are kept at a temperature of 6.0 K in a helium exchange-gas cryostat, with a voltage of 1.5 V applied in the forward direction (zero electric field). The photoluminescence under pulsed non-resonant optical excitation shows a *long* rise time, reaching its maximum after > 150 ps. The time-integrated, low-intensity luminescence shows a free-exciton line at 801.4 nm (2-meV linewidth, ≤ 0.8 -meV Stokes shift) and a weak bound-exciton line at 803.3 nm. Since both samples show a similar behavior, we restrict ourselves in the following to results obtained from sample *A*.

Optical pulses of 1.4-ps duration and of typically 0.9-nm spectral width, tunable from 720 to 840 nm, are obtained from a mode-locked Ti-sapphire laser. Reflected DFWM measurements¹⁷ are performed under weak optical excitation in resonance with the heavy-hole exciton by focusing two pulses with field vectors \mathbf{E}_1 and \mathbf{E}_2 , respectively, onto the sample with a focus diameter of about 300 μm . The stray light is reduced by placing a pinhole in the direction of the self-diffracted emission, as indicated schematically in Fig. 1. The signal is spectrally dispersed in a spectrometer of 34-cm focal length and a 300-lines/mm grating. Temporal resolution of about 7 ps (full width at half maximum) is obtained by placing a synchroscan streak camera behind one of the two exit ports of the spectrometer. The time-integrated DFWM signal is measured using a photodetector located at the other exit port. The experimental setup allows a suppression of the wrong polarization by a factor of about 100 for linearly polarized beams, limited by the cold window of the cryostat, and a factor of > 20 for circularly polarized beams.

Figure 2(a) shows a series of streak camera traces obtained for different time delays τ between the two pump pulses, generating about $2 \times 10^8 \text{-cm}^{-2}$ excitons per QW. The first two pulses of these three-pulse transients arise from the stray light of the pump beams. The third pulse is the photon echo. The time delay between the photon echo and the second pulse approximately equals τ . As shown in the inset, the intensity of the echo component depends exponentially on τ . From the experimental decay constant τ_0 with respect to τ we obtain a homogeneous dephasing time^{1,21} of $T_{2h} = 4\tau_0 = 30.4$ ps.

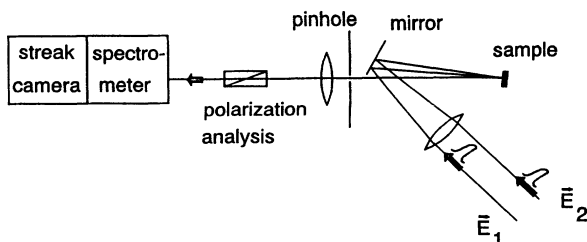


FIG. 1. Schematics of the experimental reflected two-pulse DFWM setup.

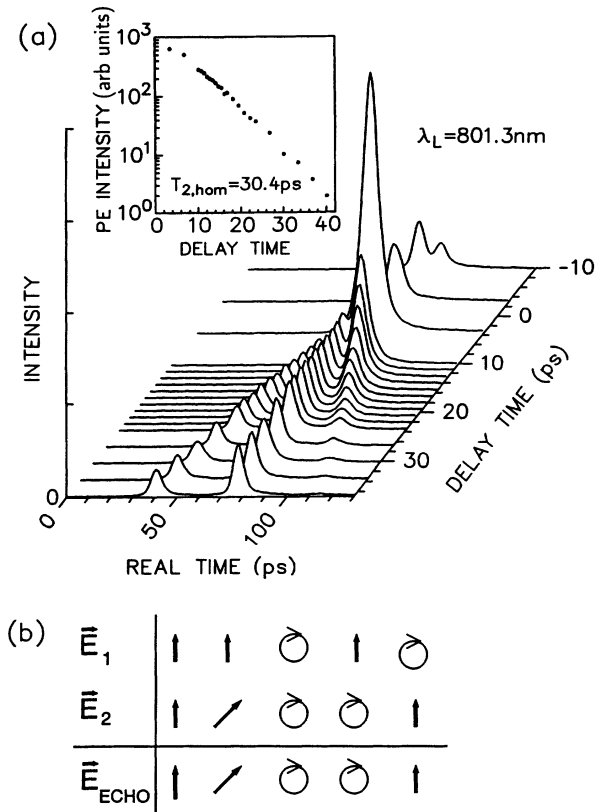


FIG. 2. (a) Streak camera traces for different time delays τ between copolarized pump pulses. The time position (78 ps) of the second pump pulse is kept constant. For positive delay time, the third pulse is formed by the PE. The inset shows the δt dependence of the numerically integrated PE intensity. (b) Dependence of the field polarization \mathbf{E}_{Echo} of the PE radiation on linear-circular field polarizations \mathbf{E}_1 and \mathbf{E}_2 of the pump beams (schematically).

The temporal isolation of the PE component of the DFWM signal now allows us to determine the dependence of the PE polarization on the polarization directions of the pump beams. The results are summarized in Fig. 2(b). Within the accuracy of the experimental setup, the PE polarization was observed to coincide with the polarization direction of the second pump beam.

No delayed signal is observed for cross-polarized pump beams. One possible interpretation of this result might be obtained from the fact that copolarized pump beams generate a long-lived (> 100 ps) population grating,¹⁶ while cross-polarized pump beams only generate an orientational grating, which decays within the dephasing time T_2 itself,¹⁶ thus suppressing self-diffraction for the delayed PE signal. However, this argument cannot explain that the observed PE polarization is *parallel* to the second pump beam, also for a 45° polarization difference between the pump beams, i.e., in spite of the presence of a population grating [see Fig. 2(b)]. We therefore conclude that the delayed signal (the PE) for cross-polarized pump beams is *already suppressed by polarization selection rules*, which are to be determined.

For further study of the polarization rules, we mea-

sured the time-integrated DFWM signal for different polarization configurations. For $0^\circ/90^\circ/0^\circ$, the signal is polarized parallel to the *first* pump pulse. Some results for 801.0-nm excitation are plotted in Fig. 3. The DFWM signal for cross-polarized pump beams (dashed curve) shows a short decay time τ_0 (≈ 2 ps) and is polarized parallel to the *first* excitation pulse. Time-resolved measurements indicate that the signal is prompt with respect to the second pump pulse [in agreement with the results of Ref. 19], corresponding to a FPD of a homogeneously broadened transition. Here the dephasing time²¹ is $T_2 = 2\tau_0 = 4$ ps. In contrast, for $0^\circ/45^\circ/90^\circ$ (full curve), the decay of the DFWM signal is significantly slower than the FPD, thus indicating a PE component. For $0^\circ/45^\circ/-45^\circ$ (not shown in Fig. 3), the signal shows the features of the FPD (similar to the dashed curve in Fig. 3) since the PE is suppressed.

Due to the different delay-time dependence of the time-integrated PE and FPD signals, an experimental distinction between these DFWM components can be made. This is exploited in the following to study the polarization rules of the FPD signal. Since the FPD signal under the conditions of Fig. 3 is typically an order of magnitude smaller than the PE, it is difficult to detect the FPD under the simultaneous presence of the PE. Therefore, we use in the following a higher excitation density (about $5 \times 10^8 \text{ cm}^{-2}$ per QW), in order to obtain FPD and PE signals of comparable strengths through a partial saturation of the PE.¹⁹

Figure 4 shows typical results obtained at 45° excitation angle. For $45^\circ/0^\circ/90^\circ$, the DFWM signal shows a two-component decay, indicating the presence of a strong FPD (fast component) and a weak PE (slow component). The presence of the PE in this forbidden geometry suggests that the DFWM polarization rules are partially relaxed under these conditions. A possible explanation for such behavior will be given below. For $45^\circ/0^\circ/0^\circ$, the PE is enhanced by an order of magnitude and there is no indication of FPD. The data for $45^\circ/0^\circ/45^\circ$ and $45^\circ/0^\circ/-45^\circ$ indicate that both components are present at $\pm 45^\circ$ detection angle. Therefore, the polarization an-

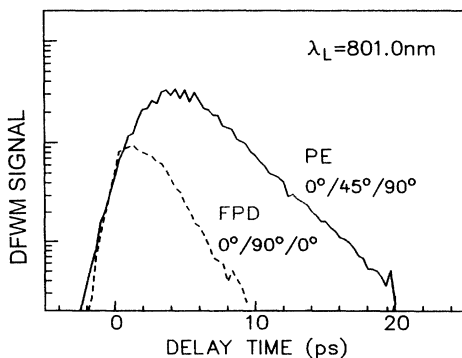


FIG. 3. Time-integrated DFWM signal (logarithm scale) vs time delay at 801.0-nm excitation wavelength and $2 \times 10^8 \text{ cm}^{-2}$ excitation density. The polarization directions (first pulse—second pulse—analyzer) are indicated. 0° corresponds to linear-electric-field polarization normal to the plane of incidence, parallel to the (110) direction of the sample.

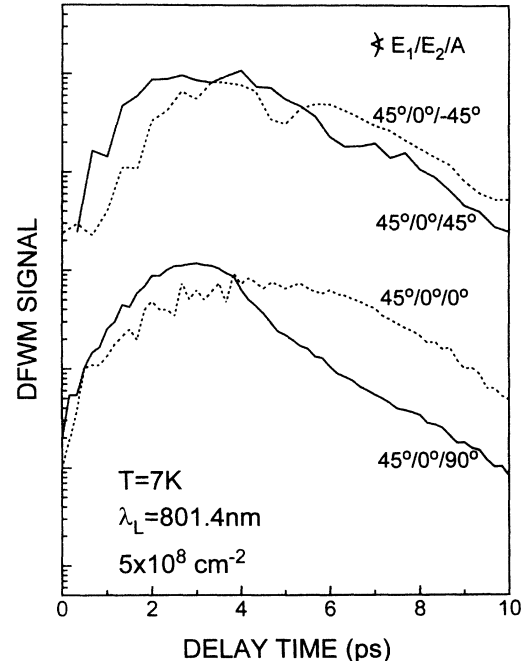


FIG. 4. Time-integrated DFWM signal (logarithm scale) vs time delay at 801.4-nm excitation wavelength and $5 \times 10^8 \text{ cm}^{-2}$ excitation density and different polarization directions as indicated. The data for $45^\circ/0^\circ/45^\circ$ and $45^\circ/0^\circ/-45^\circ$ are vertically shifted by two decades, with respect to those for $45^\circ/0^\circ/0^\circ$ and $45^\circ/0^\circ/90^\circ$.

gles for the FPD and the PE are approximately 90° and 0° , respectively, for $E_1 \parallel 45^\circ$ and $E_2 \parallel 0^\circ$.

For $45^\circ/0^\circ/-45^\circ$ (Fig. 4), the dip at 4.8 ps is attributed to a beating behavior. The beats are more pronounced for excitation at the low-energy part of the exciton distribution. The suppression of the signal at around 2 ps (with respect to the $45^\circ/0^\circ/45^\circ$ case) suggests a beat period of 2.5–3.0 ps. This value is twice as large as the expected period of quantum beats between free and bound excitons, although it agrees with the period of such beats as observed by Leo *et al.* in a 17-nm GaAs QW. Further experiments will be necessary to check whether these beats are associated with biexcitons, as has been observed by Lovering *et al.*¹¹ for a 10-nm well width under similar excitation densities.

III. THEORY

We now give a theoretical explanation of the observed polarization rules associated with the PE and FPD components. Our calculation is based on the model by Bennhardt *et al.*,¹⁴ originally formulated for a three-level system (heavy and light excitons), which we restrict to the two-level case. The model relies on the assumption that there is a coherent coupling between two degenerate electron levels or hole levels. We point out that both possibilities (the former case is probably dominant due to the smaller effective mass of the electrons) give rise to the same polarization rules, since the uncoupled electron states and hole states of the QW have the same in-plane

symmetry. As in Ref. 14, the calculation is carried out for hole coupling.

For the disorder-induced interaction H_{dis} between the spin-up and spin-down heavy-hole states, we assume the most general form,

$$H_{\text{dis}} = \begin{pmatrix} c+a & b^* \\ b & c-a \end{pmatrix}. \quad (1)$$

The parameter c describes the inhomogeneous broaden-

ing²¹ induced by a long-range disorder. The parameters a (real) and b (complex) are introduced to take into account short-range disorder (i.e., within the length scale of the Bohr radius), which splits these states by the energy $\pm d \equiv \pm\sqrt{a^2 + bb^*}$ and changes their symmetry. Following the calculation of Ref. 14, we assume $\mathbf{E}_2 = E_2 \mathbf{e}_x$ polarized in the x direction, and $\mathbf{E}_1 = E_1 (\mathbf{e}_x \cos\phi + \mathbf{e}_y \sin\phi)$ at an angle ϕ with respect to \mathbf{E}_2 , with unit vectors $\mathbf{e}_x, \mathbf{e}_y$. In the limit $\mathbf{E}_1(t) \sim \delta(t-\tau)$ and $\mathbf{E}_2(t) \sim \delta(t)$, we obtain the following third-order polarization in the diffracted direction $2\mathbf{k}_2 - \mathbf{k}_1$:

$$\mathbf{P}_{2\mathbf{k}_2 - \mathbf{k}_1}^3 = -\frac{i}{2} |\mu|^4 \theta(\tau) \theta(t-\tau) E_2^2 E_1^* e^{-i(\epsilon_{cv} + c)(t-2\tau)} e^{-\gamma_h t} \times \begin{pmatrix} \cos[d(t-2\tau)] \cos\phi - \frac{a}{d} \sin[d(t-2\tau)] \sin\phi \\ -\frac{a}{d} \sin[d(t-2\tau)] \cos\phi - \frac{a^2}{d^2} \cos[d(t-2\tau)] \sin\phi - \frac{2bb^*}{d^2} \cos(dt) \sin\phi \end{pmatrix}, \quad (2)$$

with the dipole moment $|\mu|$, the energy ϵ_{cv} of the unperturbed transition, and the damping constant (homogeneous dephasing rate) γ_h . We note that the cases $b=0$ and $a=0$ correspond to the polarization rules for heavy-hole transitions obtained in Refs. 12 and 14, respectively.

It is instructive to determine the nonlinear polarization for some simple inhomogeneous distributions of H_{dis} . If the short-range distribution is symmetric in a with respect to $a=0$, the terms linear in a cancel out in Eq. (2). Assuming independent Gaussian distributions $\sim \exp(-c^2/\gamma_c^2)$ and $\sim \exp(-d^2/\gamma_d^2)$, respectively, with the inhomogeneous broadenings γ_c^{-1} and γ_d^{-1} for the long-range and short-range disorder (note that $d \geq 0$), the resulting polarization reads

$$\mathbf{P}_{2\mathbf{k}_2 - \mathbf{k}_1}^3 = -\frac{i}{2} |\mu|^4 \theta(\tau) \theta(t-\tau) E_2^2 E_1^* e^{-i\epsilon_{cv}(t-2\tau)} e^{-\gamma_h t} e^{-(t-2\tau)^2 \gamma_c^2 / 4} \times \left[e^{-(t-2\tau)^2 \gamma_d^2 / 4} \begin{pmatrix} \cos\phi \\ -\frac{a^2}{d^2} \sin\phi \end{pmatrix} + e^{-t^2 \gamma_d^2 / 4} \begin{pmatrix} 0 \\ -\frac{bb^*}{d^2} \sin\phi \end{pmatrix} \right], \quad (3)$$

provided that $a/d = \text{const}$ within the entire distribution. A variation of a/d will result in an inhomogeneous distribution of polarization rules, giving rise to a depolarization of the signal. The measured DFWM intensity is proportional to the square amplitude of the nonlinear polarization component parallel to the analyzer.

IV. DISCUSSION

Within this model, both the short-range and long-range disorder give rise to a delayed signal (PE), centered at $t \approx 2\tau$, which allows us to determine the *homogeneous* contribution γ_h to the dephasing process,²¹ corresponding to four times the decay constant of the time-integrated DFWM intensity with respect to τ . In inhomogeneously broadened systems, the prompt contribution (FPD), centered at $t \approx \tau$, is attenuated with respect to the PE by a factor of about $\exp[-\tau^2(\gamma_c^2 + \gamma_d^2)/2]$. Therefore, it decays faster with respect to τ than the PE. This means, in particular, that the decay of the FPD component is due to the combined action of the *homogeneous and inhomogeneous dephasing rates*. In the presence of short-range disorder, both the homogeneous and the inhomogeneous broadenings of the excited exciton popula-

tion can be determined from a simultaneous measurement of the two DFWM components.

It is in principle possible to distinguish between short-range and long-range disorder in a time-resolved DFWM experiment, since only short-range disorder should produce two DFWM components with different time dependence. In addition, the ‘‘FPD’’ component [i.e., the y -polarized term in Eq. (3)] is centered at $t \approx \tau$ for $\gamma_c < \gamma_d$, and at $t \approx 2\tau$ for $\gamma_c \gg \gamma_d$. The absence of short-range disorder manifests itself in equal signal intensities of the two components (e.g., under cross-polarized and copolarized excitation, respectively), and in polarization-independent dephasing times.

In realistic QW structures, we expect less idealized exciton distributions. Here γ_h usually depends on energy, with larger homogeneous broadening at the high-energy part of the exciton distribution. In addition, the degree of symmetry breaking [i.e., the ratio between a and b in Eq. (1)] is supposed to increase at decreasing energy, corresponding to disorder-induced localization. Finally, an intensity dependence of the symmetry properties results from different saturation properties of the individual excitons. Even in the highest-quality QW's, these distributions also depend on the well width. Further, we note

that the model still predicts equal DFWM signal intensities at $\tau=0$ under cross-polarized and copolarized excitation, which is in contrast to some observations.^{14,15} This suggests that additional mechanisms, like excitation-induced dephasing,¹⁵ are also of importance in QW systems.

Applying these considerations to the present experiments, the observation of both an FPD and a PE component provides clear evidence of short-range disorder. Long-range disorder of the optically excited exciton distribution is weak, since the FPD component still has a significant intensity. We note, however, that the exciton distribution under study depends critically on the spectral narrowness and on the precise wavelength of the excitation. The observed polarization rules agree with the theoretical ones, with signal polarizations of the FPD and the PE components orthogonal and essentially parallel to E_2 , respectively. This implies in particular $|a| \ll |b|$. In addition, the data for $45^\circ/0^\circ/90^\circ$ (Fig. 4) suggest a finite (but small) value of $|a/b|$. More detailed experiments will be necessary to quantify these values.

Using Eq. (3), the measured τ -dependent change of the intensity ratio between the time-integrated PE and FPD, typically one order of magnitude at $\Delta\tau \approx 6$ ps, allows us to estimate the inhomogeneous broadening γ_d of the excited exciton distributions, with the result $\gamma_d^{-1} = 2-3$ ps. This value of γ_d is consistent with both the value expected from the luminescence linewidth of the QW excitons and the spectral width of the laser pulse. Finally, we note that the above phenomenological model might still be controversial, since a microscopic calculation of the broken-exciton symmetry (e.g., due to short-range well-width fluctuations) does not yet exist.

V. CONCLUSION

We have shown that the diffracted signal in two-pulse DFWM by heavy-hole excitons in quantum wells generally contains two components (PE and FPD) with different polarization properties and different time dependences, both in real time and in delay time. We have studied the time dependence and polarization rules of these components in time-resolved and polarization-resolved experiments. Theoretical considerations show that such two-component behavior is a direct consequence of *short-range disorder*, and that short-range disorder can be distinguished from long-range disorder in DFWM experiments. The dephasing time determined from the PE corresponds to the *homogeneous* dephasing time, while the FPD is related to the combined *homogeneous and inhomogeneous* dephasing.

Note added. We recently became aware of a paper by Bott *et al.*,²³ explaining the observed DFWM intensity difference for cross-polarized–copolarized excitation and the density dependence of DFWM polarization rules in terms of exciton-exciton interaction.

ACKNOWLEDGMENTS

The authors are grateful to P. Koidl for the encouragement of this study and to H. S. Rupprecht for continuous support of the work at Freiburg. We also thank K. Schwarz for expert technical assistance. Part of the work at Stuttgart was sponsored by the Bundesministerium für Forschung und Technologie (Germany).

*Present address: Paul-Drude-Institut für Festkörperelektronik, Hausvogteiplatz 5-7, D-10117 Berlin, Germany.

¹L. Schultheis, M. D. Sturge, and J. Hegarty, *Appl. Phys. Lett.* **47**, 995 (1985).

²L. Schultheis, J. Kuhl, A. Honold, and C. W. Tu, *Phys. Rev. Lett.* **57**, 1635 (1986).

³L. Schultheis, A. Honold, J. Kuhl, J. Köhler, and C. W. Tu, *Phys. Rev. B* **34**, 9027 (1986).

⁴D.-S. Kim, J. Shah, J. E. Cunningham, T. C. Damen, W. Schäfer, M. Hartmann, and S. Schmitt-Rink, *Phys. Rev. Lett.* **68**, 1006 (1992).

⁵J.-Y. Bigot, M. T. Portella, R. W. Schönlein, and C. V. Shank, *Phys. Rev. Lett.* **67**, 636 (1991).

⁶D.-S. Kim, J. Shah, J. E. Cunningham, T. C. Damen, S. Schmitt-Rink, and W. Schäfer, *Phys. Rev. Lett.* **68**, 2838 (1992).

⁷E. O. Göbel, K. Leo, T. C. Damen, J. Shah, S. Schmitt-Rink, W. Schäfer, J. F. Müller, and K. Köhler, *Phys. Rev. Lett.* **64**, 792 (1990).

⁸K. Leo, T. C. Damen, J. Shah, and K. Köhler, *Phys. Rev. B* **42**, 11 359 (1990).

⁹K. Leo, J. Shah, E.-O. Göbel, T. C. Damen, K. Köhler, and P. Ganser, *Appl. Phys. Lett.* **56**, 2031 (1990); *Superlatt. Microstruct.* **7**, 427 (1990); K. Leo *et al.*, *Phys. Rev. Lett.* **66**, 201 (1991).

¹⁰K. Leo, M. Wegener, J. Shah, D. S. Chemla, E.-O. Göbel, T. C. Damen, S. Schmitt-Rink, and W. Schäfer, *Phys. Rev. Lett.* **65**, 1340 (1990).

¹¹D. J. Lovering, R. T. Phillips, G. J. Denton, and G. W. Smith, *Phys. Rev. Lett.* **68**, 1880 (1992).

¹²S. Schmitt-Rink *et al.*, *Phys. Rev. B* **46**, 10 460 (1992).

¹³R. Eccleston, J. Kuhl, D. Bennhardt, and P. Thomas, *Solid State Commun.* **86**, 93 (1993).

¹⁴D. Bennhardt, P. Thomas, R. Eccleston, E. J. Mayer, and J. Kuhl, *Phys. Rev. B* **47**, 13 485 (1993).

¹⁵H. Wang, K. Ferrio, D. G. Steel, Y. Z. Hu, R. Binder, and S. Koch, *Phys. Rev. Lett.* **71**, 1261 (1993).

¹⁶L. Schultheis, J. Kuhl, A. Honold, and C. W. Tu, *Phys. Rev. Lett.* **57**, 1797 (1986).

¹⁷A. Honold, L. Schultheis, J. Kuhl, and C. W. Tu, *Appl. Phys. Lett.* **52**, 2105 (1988).

¹⁸G. Noll, U. Siegner, S. G. Shevel, and E. O. Göbel, *Phys. Rev. Lett.* **64**, 792 (1990).

¹⁹S. T. Cundiff, H. Wang, and D. G. Steel, *Phys. Rev. B* **46**, 7248 (1992).

²⁰M. D. Webb, S. T. Cundiff, and D. G. Steel, *Phys. Rev. Lett.* **66**, 934 (1991).

²¹T. Yajima and Y. Taira, *J. Phys. Soc. Jpn.* **47**, 1620 (1979).

²²H. Schneider, K. v. Klitzing, and K. Ploog, *Superlatt. Microstruct.* **5**, 383 (1989); *Europhys. Lett.* **8**, 575 (1989); H. Schneider, W. W. Rühle, K. v. Klitzing, and K. Ploog, *Appl. Phys. Lett.* **54**, 2656 (1989).

²³K. Bott, O. Heller, D. Bennhardt, S. T. Cundiff, P. Thomas, E. J. Mayer, G. O. Smith, R. Eccleston, J. Kuhl, and K. Ploog, *Phys. Rev. B* **48**, 17 418 (1993).